Eur. Phys. J. Spec. Top. (2024) 233:903–912
https://doi.org/10.1140/epjs/s11734-024-01094-6

THE EUROPEAN PHYSICAL JOURNAL SPECIAL TOPICS

Regular Article

Isomeric decays with multipolarity $\lambda \geq 3$

Zsolt Podolyák[a]

Department of Physics, University of Surrey, Guildford GU2 7XH, UK

Received 1 December 2023 / Accepted 11 January 2024 / Published online 31 January 2024

Abstract Isomeric decays with multipolarity $\lambda \geq 3$ are discussed. Parity changing $E3$, $M4$, $E5$ decays are more widespread within the nuclide chart when compared to parity conserving $M3$, $E4$ and $M5$ transitions, which is the consequence of the properties of the nuclear shell model. The $E3$ transitions around ^{208}Pb are classified depending on their origins. Systematics of $M4$ and $E5$ transitions are presented. These provide an excellent test to the study of shell evolution in different parts of the nuclide chart as well as the nature of the effective charges.

1 Introduction

Isomeric (or metastable) states are long-lived nuclear excitations. There is no a clear definition of what constitute an isomer. Often states with half-lives longer than a limit of 10 ns or 100 ns are considered isomeric. For example, the latest *Atlas of nuclear isomers* [1] published in 2023 uses the $T_{1/2} = 10$ ns limit. The definition of isomerism does not require any hindrance of the decay related to the structure of the states involved. For a detailed discussion of isomerism in nuclei, including types of isomers, see [2].

The Weisskopf γ-ray half-life (which is the partial half-life) estimate is based on an extreme single-particle approximation. It depends very strongly on the multipolarity λ, e.g. the angular momentum carried by the photon: $T^W_{1/2} \sim E^{-(2\lambda+1)}$ (see Fig. 1), where E is the transition energy. Consequently, transitions with large multipolarity have large partial half-lives. They are relatively rare, as low multipolarity transitions usually dominate. When an excited state cannot decay by low multiplicity photons due to lack of lower lying state with similar spin, large multipolarity decays are the only internal decays possible. This leads to long-lived isomeric states. As a general rule, the excited nuclear states decaying by transitions of multipolarity $\lambda \geq 4$ are isomeric. This is valid also for magnetic $\lambda = 3$ $M3$ transitions. In case of $E3$ decays, the situation is more complex: the isomerism of the state depends on the collectivity of the decay, and strongly on its energy (and the definition of isomer). Isomeric states can often decay also by charged particle decays, not only internally. Consequently, the majority of internally decaying long-lived isomers are in nuclei close to stability.

The Weisskopf hindrance factor can be expressed as: $F_W = T^\gamma_{1/2}/T^W_{1/2}$, where $T^\gamma_{1/2}$ is the partial γ-ray half-life, which is determined experimentally. Not only the size of the angular momentum, but also its orientation is conserved, which is relevant in the case of deformed nuclei. Here, the K quantum number is the projection of the total angular momentum on the symmetry axis. For K isomers (where in the isomeric state the angular momentum is generated by unpaired nucleons, therefore $I{=}K$), the reduced hindrance is defined as $f_\nu = F_W^{1/\nu}$, where the degree of K forbiddenness is $\nu = \Delta K - \lambda$.

Excited states usually decay with γ-ray transitions of low multipolarity. As the multipole order increases, the number of known cases decreases rapidly. Throughout this article, we use a lot of experimental nuclear data. As a rule, these are taken from the ENSDF compilation (reference [3]), and this is not explicitly referenced at each place. However, the newer articles not in the compilations are explicitly referenced.

Internal γ decays are governed by one-body operators. Consequently only the quantum number of a single nucleon can change, whilst the others act as spectators. The spherical shell-model single-particle orbitals are shown in Fig. 2. The strongest transitions (*i.e.* largest reduced transition strengths) with multiplicity λ are expected between orbitals with $\Delta l = \Delta j = \lambda$. Transitions are allowed also for other orbital pairs, but generally

[a] e-mail: z.podolyak@surrey.ac.uk (corresponding author)

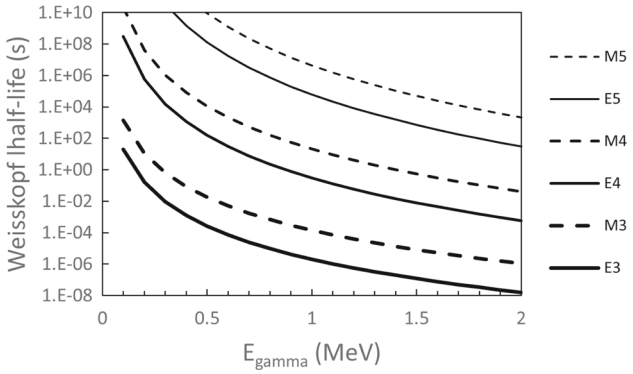

Fig. 1 Weisskopf single-particle partial γ-ray half-live estimates for mass A = 100. Note that the electron conversion is not considered

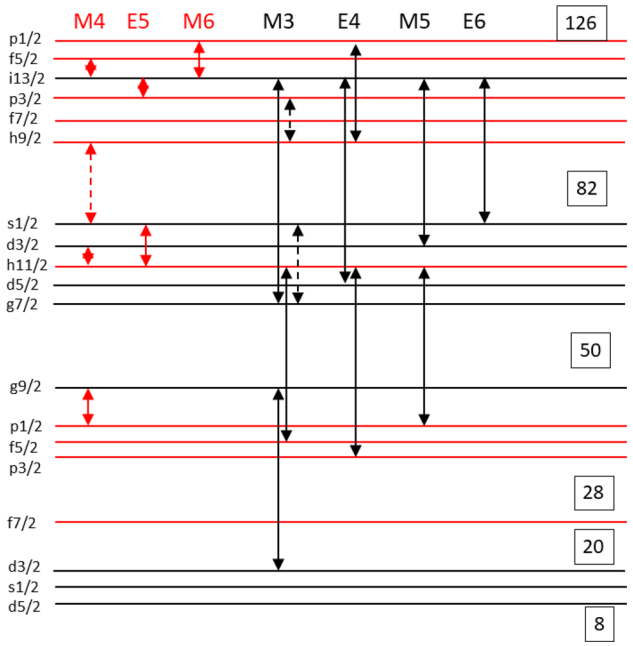

Fig. 2 Shell-model single-particle orbitals between magic numbers 8 and 126. Positive parity orbitals are indicated in black, whilst negative-parity ones are in red. The stretched $\Delta j = \lambda$ orbital pairs for $M3$, $E4$, $M4$, $E5$, $M5$, $E6$, $M6$ are connected with arrows, red for parity changing transitions and black for parity conserving ones. Arrows with dashed lines indicate l-forbidden transitions. See text for details

these are weaker due to the values of the angular momentum coupling constants. In Fig. 2, the stretched $\Delta j = \lambda$ orbital pairs for $M3$, $E4$, $M4$, $E5$, $M5$, $E6$, $M6$ transitions are indicated with arrows. One notes that parity changing $M4$ and $E5$ transitions can be found within the same shell (therefore the transitions are of low energy), which can result in long-lived isomeric states. In contrast, parity conserving stretched $M3$, $E4$ and $M5$ transitions usually connects far lying orbitals, and consequently there are many other decay channels open and these will not be isomeric. Or when they are in the same shell, the transitions are l forbidden. The consequence of this is that parity changing $\lambda \geq 3$ are more abundant than partiy conserving ones. The ENSDF compilation [3] lists about $\sim$1000 stretched $E3$ compared to $\sim$100 $M3$ decays. Similarly, the numbers for observed $M4/E4$ and $E5/M5$ decays are 121/34 and 17/1, respectively.

2 E3 decays around ^{208}Pb

There is a large number of $E3$ transitions observed. They are not all isomeric, depending mainly on their energy, but also on whether they are of collective nature. The discovery of isomerism [4] itself involves an $E3$ decaying

isomer in ^{234}Pa, and it is attributed to Otto Hahn [5]. Isomeric $E3$ transitions were observed over a large part of the nuclide chart, as shown in Fig. 10 of [1]. Here we will focus on the $E3$ transitions around the doubly magic ^{208}Pb nucleus. Similar concepts and logic could be applied to other parts of the nuclide chart.

The single-particle proton and neutron orbitals around $^{208}_{82}\mathrm{Pb}_{126}$ are shown in Fig. 3. The first excited state in ^{208}Pb at 2.614 MeV has spin-parity 3^- and a large $B(E3; 3^- \rightarrow 0^+)$= 33.8(6) W.u. transition strength to the ground state. It is, therefore, a collective state, interpreted to be the consequence of a large number of Δl=Δj=3 orbital pairs across the $Z = 82$ and $N = 126$ shell gaps, shown by arrows in Fig. 3. Other orbital pairs also contribute for the composition of the collective octupole phonon see [6]. Consequently, shell model calculations incorporating full shells around $Z = 82$ (covering 50–126) and $N = 126$ (82–184) reproduce well the properties of this 3^- state and other collective states in ^{208}Pb [7] and neighbouring [8–10] nuclei.

Nuclei in the vicinity of ^{208}Pb exhibit also non-collective octupole decays which are linked to individual orbital pairs within the same shell. As a consequence of the spin–orbit coupling, un-natural parity high-j orbitals are present in each shell around $Z = 82$ and $N = 126$, and these form pairs with opposite parity orbitals which can give rise to $E3$ transitions. These are indicated for both $\Delta l = \Delta j = 3$ (in red), and Δl=1, $\Delta j = 2$ (in blue) pairs

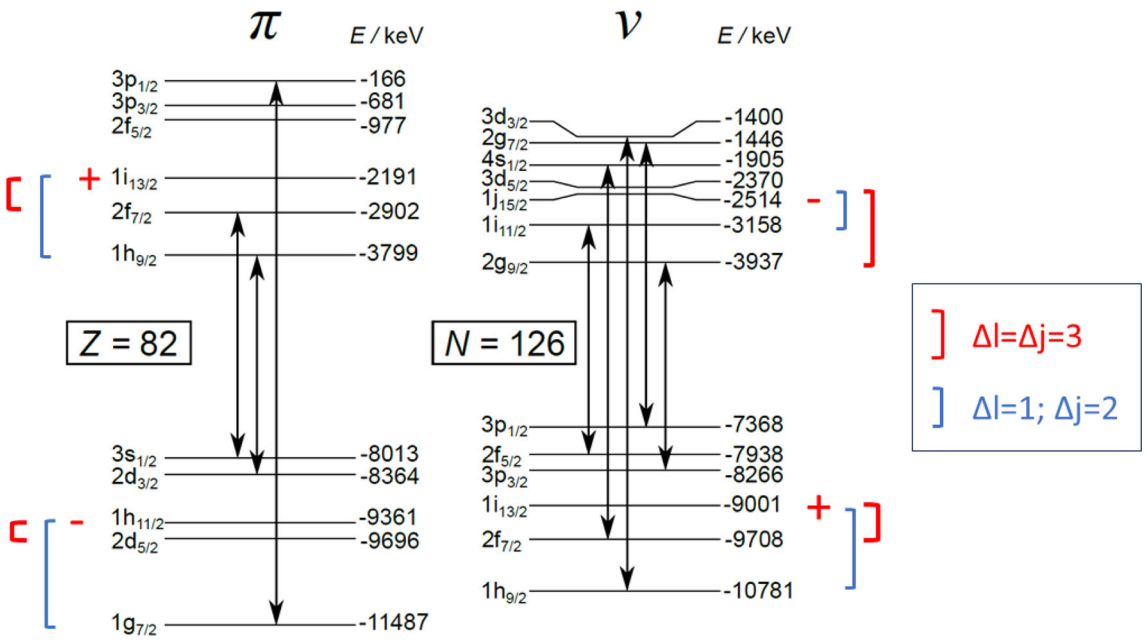

Fig. 3 Single-particle orbitals around the doubly magic nucleus ^{208}Pb. In each shell, orbital pairs which can give rise to $E3$ transitions are indicated, separately for $\Delta l = 3$ (in red) and $\Delta l = 1$ (in blue) pairs. In addition, $\Delta j = \Delta l = 3$ pairs from adjacent shells are connected with black arrows

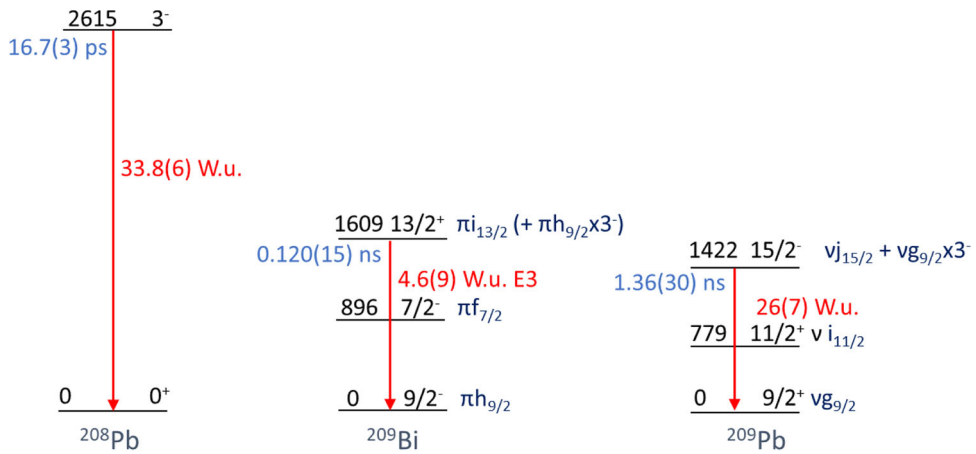

Fig. 4 Collective E3 decay in doubly magic ^{208}Pb, as well as single-particle governed ones in one-valence particle nuclei ^{209}Bi and ^{209}Pb

in Fig. 3. First, we examine the one-valence particle/hole nuclei. In the one proton-particle ^{209}Bi, the $\pi i_{13/2}$ state is yrast and can decay into the $\pi f_{7/2}$ and $\pi h_{9/2}$ states via stretched and un-stretched $E3$ transitions, respectively. Due to the energy factor, only the $i_{13/2} \rightarrow h_{9/2}$ transition was observed and its $E3$ component has a transition strength of $B(E3) = 4.6(9)$ W.u. [11]. This relatively modest strength is a consequence of being an un-stretched transition, but it is also boosted by the $\pi h_{9/2} \times 3^-$ component of the wave function of the predominantly $\pi i_{13/2}$ state (3^- is the collective octupole phonon), as shown in Fig. 4. In the one neutron-particle ^{209}Pb nucleus, the situation is slightly different. The $\nu j_{15/2}$ state is yrast and can decay into the $\nu g_{9/2}$ and $\nu i_{11/2}$ states via stretched and un-stretched $E3$ decays, respectively. In this case, the energy factor favours the stretched $E3$ and only this one was observed. Its strength is rather large at 26(7) W.u. This is due to its $\Delta j = \Delta l = 3$ nature and the octupole phonon admixture into the $\nu j_{15/2}$ dominated state (see Fig. 4). In the shells below $Z = 82$ and $N = 126$, $E3$ transitions are mediated by the $\pi h_{11/2}$ and $\nu i_{13/2}$ orbitals, respectively, paired with orbitals which are not yrast (Fig. 3). As a consequence in ^{207}Tl and ^{207}Pb, no $E3$ transitions were observed connecting the relevant single-particle states.

For a better understanding of the origin of the $E3$ decays in the region, Fig. 5 presents the sytematics of these decays for the Z=82 isotopes and $N = 126$ isotones. In lead isotopes with $N < 126$, all observed $E3$ decays have transition strengths of $B(E3) < 1$ W.u. These are mediated by the $i_{13/2} - f_{7/2}$ neutron orbitals. The low strengths are the consequence of the non-yrastness of the $\nu f_{7/2}$ orbital, meaning that the isomeric states (which are based on the high-j $i_{13/2}$ orbital) decay into a level where the $f_{7/2}$ orbital provides a minor part of the wave function. In contrast, the $B(E3)$ values for $N > 126$ lead isotopes are large [12]. These are mediated by the $j_{15/2} - g_{9/2}$ neutron-orbital pair. ^{208}Pb itself has an $I^\pi = 23^+$ isomer mediated by the same transition [13], in addition to the (non-isomeric) collective 3^-. One notes that the largest $B(E3)$ value for neutron-deficient Pb nuclei is the $B(E3; 7^- \rightarrow 4^+) = 0.7(3)$ W.u. in ^{202}Pb. The large uncertainty relates to the branching ratio and this would merit revisiting.

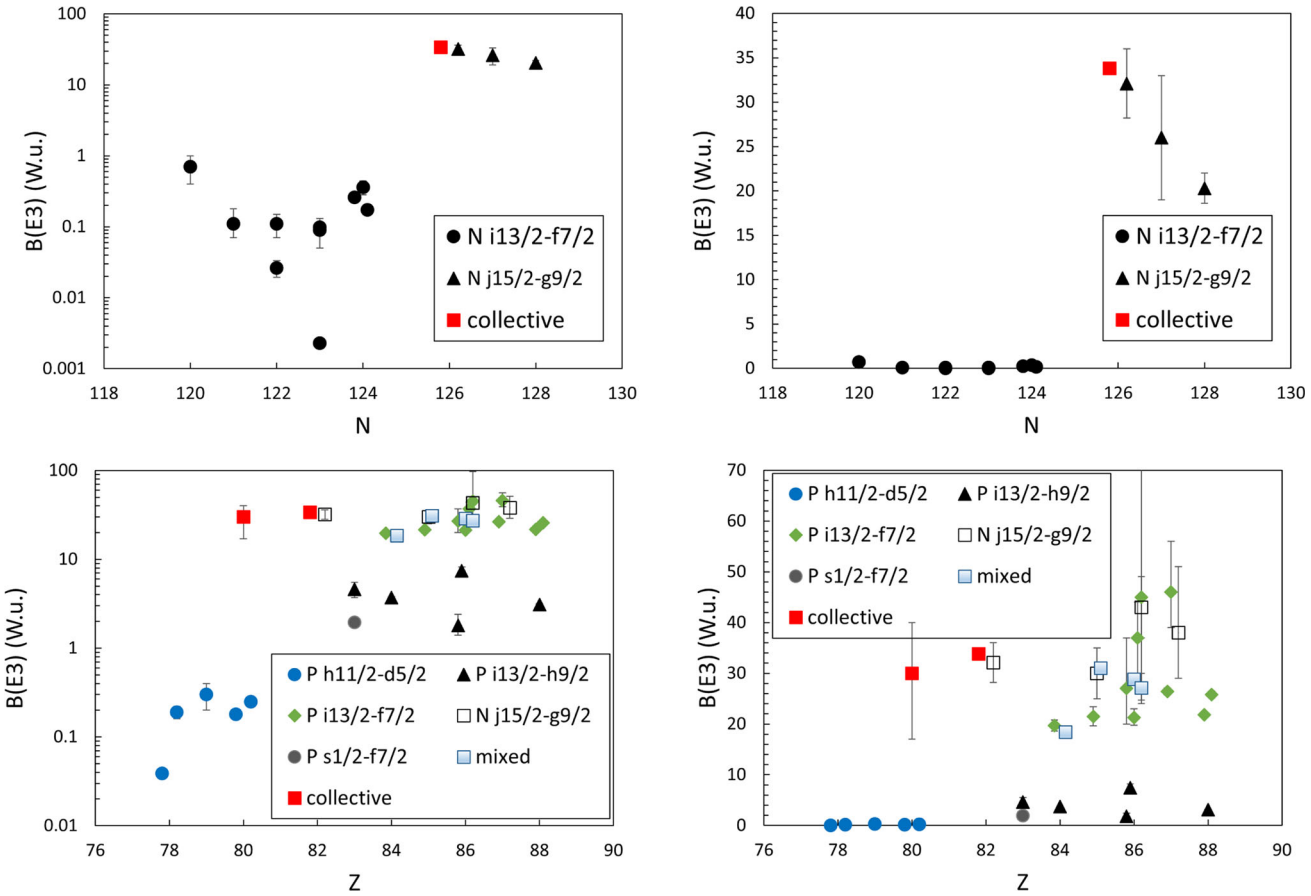

Fig. 5 Systematics of $E3$ transitions in (*top*) $Z = 82$ and (*bottom*) $N = 126$ nuclei. The origins of the transitions are indicated. The pictures side by side present the same data, using (*left*) logarithmic and (*right*) linear y axes. See the text for details

$N = 126$ isotones below ^{208}Pb exhibit isomeric $E3$ decays governed by the $\pi h_{11/2} - d_{5/2}$ transition (Fig. 5). These were observed in ^{206}Hg, ^{205}Au and ^{204}Pt with $B(E3)$ <1 W.u. [14]. The low value is because the $\pi d_{5/2}$ is not yrast, and therefore this orbital provides a minority component into the wave functions of the daughter states. In contrast, the neutron-deficient N = 126 isotones exhibit isomeric states decaying with $B(E3) > 1$ W.u. Their origins are more diverse. The proton $i_{13/2} - h_{9/2}$ mediated transitions have strengths in order of few W.u., similar to that already mentioned in ^{209}Bi. In contrast, the ones mediated by the $\Delta j = 3$ proton $i_{13/2} - f_{7/2}$ and neutron $j_{15/2} - g_{9/2}$ pairs are stronger. In some cases, small mixing can increase considerably the transition strength. This is quite common at high spins, where configuration mixing is more prevalent. For the 16^+ isomer in ^{210}Po and $39/2^-$ in ^{211}At, the main configurations suggest a $\nu i_{13/2} - h_{9/2}$ decay. However, the measured $B(E3)$ values are large, quantitatively explained [15] by wave-function admixtures which allow $\pi i_{13/2} - f_{7/2}$ and $\nu j_{15/2} - g_{9/2}$ transitions. The situation is similar for the 25^- and 30^+ isomeric states in ^{212}Rn [16]. These cases, when the large strength is determined by minority components of the wave function are labeled as mixed in Fig. 5. There is also one transition labeled as proton $s_{1/2} - f_{7/2}$, observed in ^{209}Bi. The $\pi s_{1/2}$ is an intruder from below $Z = 82$. Therefore, the $1/2^-$ state configuration is actually $\pi s^{-1}_{1/2}(h^2_{9/2})_0$, and decays into the $\pi f_{7/2}(h^2_{9/2})_0$ component of the predominantly $\pi f_{7/2}$ state. Alternatively the decay is due to the $\pi f_{7/2} \times 3^-$ component of the $1/2^-$ state. In addition to single-orbital pair mediated transitions, Fig. 5 also indicates the collective $B(E3)$ values for ^{206}Hg [8] and ^{208}Pb (these are not isomeric due to their large energy). One should note that it is not always possible to divide the $E3$ decays so neatly based on their strengths. For example, in ^{208}Pb, the 8^+ isomeric state decays into two 5^- states. Both $E3$ decays are governed by the neutron $j_{15/2} - g_{9/2}$ transition; however because of the mixing between the 5^- states, the strengths are lower than would be otherwise, at 12.3(2) W.u. and 0.71(17) W.u. [13]. Also a 28^- isomer was identified in ^{208}Pb decaying with $B(E3) = 56(7)$ W.u. The large value is likely due to two $j_{15/2}$ neutrons in the structure of the isomer [13]. These are not shown in Fig. 5. For discussions of $E3$ transitions in the vicinity of ^{208}Pb, see also [15–17]. The above exercise, namely connecting the use of the measured transition strengths to the underlying origin of the transitions, can be extended to the whole region, beyond the semi-magic nuclei discussed here.

3 M3 and E4 decays

There is no concentration of $M3$ (magnetic octupole) and $E4$ (electric hexadecapole) isomeric decays in any region of the nuclide chart (see Fig. 10 of [1]). This is a consequence of the nuclear shell model, where the low number of $M3$ decays is attributed to the fact that the $\Delta j = 3$ same parity orbital pairs are in different shells. The exceptions are the $h_{9/2} - p_{3/2}$ and $g_{7/2} - s_{1/2}$ pairs; however, in both cases, the $M3$ transitions are l forbidden. The situation is somewhat similar for $E4$ transitions, as shown in Fig. 2, in the sense that the orbitals are far in energy from each other. Therefore, $M3$ and $E4$ transitions are generally of very high energy and other, much faster, decay branches dominate.

The only stretched $M3$ transition observed connecting single particle states is in ^{113}Sn$_{63}$. Here the first excited state with $7/2^+$ $\nu g_{7/2}$ decays into the $1/2^+$ $\nu s_{1/2}$ ground state. The $B(M3) = 0.0281(15)$ W.u. transition strength is rather low, which probably is the consequence of being l forbidden ($\Delta l = 4$). Note that this transition is believed to have an $E4$ component, with the mixing ratio determined from the α_K/α_L ratio of [18]. The mixing should be remeasured as the deduced value of $B(E4) = 140(50)$ W.u. is too large [19], beyond the recommended upper limit [20].

$M3$ transitions were identified in several deformed nuclei, and they are not discussed here. There are much fewer $E4$ isomeric decays oberved. Odd-mass ^{179}W, ^{189}Os and ^{191}Os have such one-quasiparticle states. In the odd-odd ^{174}Lu, a two-quasiparticle $K^\pi = I^\pi = 6^-$ isomer with configuration $\pi 7/2[404]\nu 5/2[512]$ decays into the 2^- and 3^- members of the $K^\pi = 1^-$ rotational band built on the same, but anti-aligned configuration, with $B(M3) = 6.4(6)\times10^{-7}$ W.u. and $B(E4) = 0.00011(8)$ W.u., respectively. These correspond to very large reduced hindrance value of $f_\nu \sim 1250$ for the $M3$ and $f_\nu \sim 10^4$ for the $E4$ transition. In ^{177}Lu, a three-quasiparticle $K^\pi = I^\pi = 23/2^-$ isomer with $\pi 7/2[404]\nu 7/2[514]9/2[624]$ configuration decays by $B(M3) = 2.3(6)\times10^{-11}$ W.u and $B(E4) = 1.7(4)\times10^{-9}$ W.u. into members of the $K^\pi = 9/2^-$ $\pi 9/2[514]$ band [21, 22]. The reduced hindrance values are $f_\nu = 460(3)$ for the M3 and $f_\nu = 830(6)$ for the E4 transition [23], which are also rather large.

4 M4 decays

The orbital pairs which can give rise to stretched $M4$ (magnetic hexadecapole) transitions are $g_{9/2} - p_{1/2}$, $h_{11/2} - d_{3/2}$, $i_{13/2} - f_{5/2}$ (see Fig. 2). These are all $\Delta l = 3$, $\Delta j = 4$ pairs. First, we examine isotopic/isotonic chains at or in the immediate vicinity of magic numbers where the wave functions are expected to be the purest.

The first orbitals below the magic number 50 are $g_{9/2}$ and $p_{1/2}$. Consequently the ground state of the $Z = 49$ odd-mass indium nuclei is $9/2^+$, whilst the first excited state has spin-parity $1/2^-$. The $1/2^-$ state is isomeric, and it can decay internally through an $M4$ transition. Figure 6 shows the energy and reduced $B(M4)$ transition strength systematics. In neutron-rich indium nuclei, the isomeric state β^- decays. β decays dominate over internal decay starting from ^{115}In, whilst from ^{123}In, no internal decay was observed. On the proton-rich side of stability, in ^{103}In, $\beta^+ + EC$ decay dominates over internal decay. In ^{101}In [24] and ^{99}In [25], the $1/2^-$ states were identified in mass measurements. The transition strength and transition energy change smoothly with neutron number. Interestingly they seem to be correlated. There is one $B(M4)$ data point which seems to break the smooth changing behaviour, that at $^{117}\text{In}_{68}$. Possibly the internal decay to β decay ratio is incorrect and it should be remeasured.

Similarly, the ground state of the $N = 49$ odd-mass isotones is $9/2^+$ based on a neutron $g_{9/2}$ hole, and they have a $1/2^-$ first excited state based on $\nu p_{1/2}$. Internal $M4$ decays were observed in ^{85}Kr, ^{87}Sr, ^{89}Zr, ^{91}Mo and ^{93}Ru (see Fig. 6). On the neutron-rich side, the $1/2^+$ isomers were identified in ^{83}Se and ^{81}Ge and they β^- decay, without observed internal decay branches. On the neutron-deficient side, the energies of the $1/2^-$ isomer in ^{95}Pd, ^{97}Cd are not known. Surprisingly, its decay was observed and its lifetime measured in the more exotic ^{97}Cd [26], but not in ^{95}Pd. Similarly to the proton-rich $Z = 49$ case, these are of great interest as they give information on the evolution of single-particle states approaching doubly magic ^{100}Sn. The deduced $B(M4)$ values are constant for $Z \leq 40$ nuclei, with lower values beyond the $Z = 40$ sub-shell closure.

The $N = 81$ odd-mass isotones are characterised by a long-lived $11/2^-$ $\nu h_{11/2}$ state. This is usually the second excited state (except in neutron-rich ^{131}Sn where it is the first one), with $3/2^+$ $\nu d_{3/2}$ being the ground state

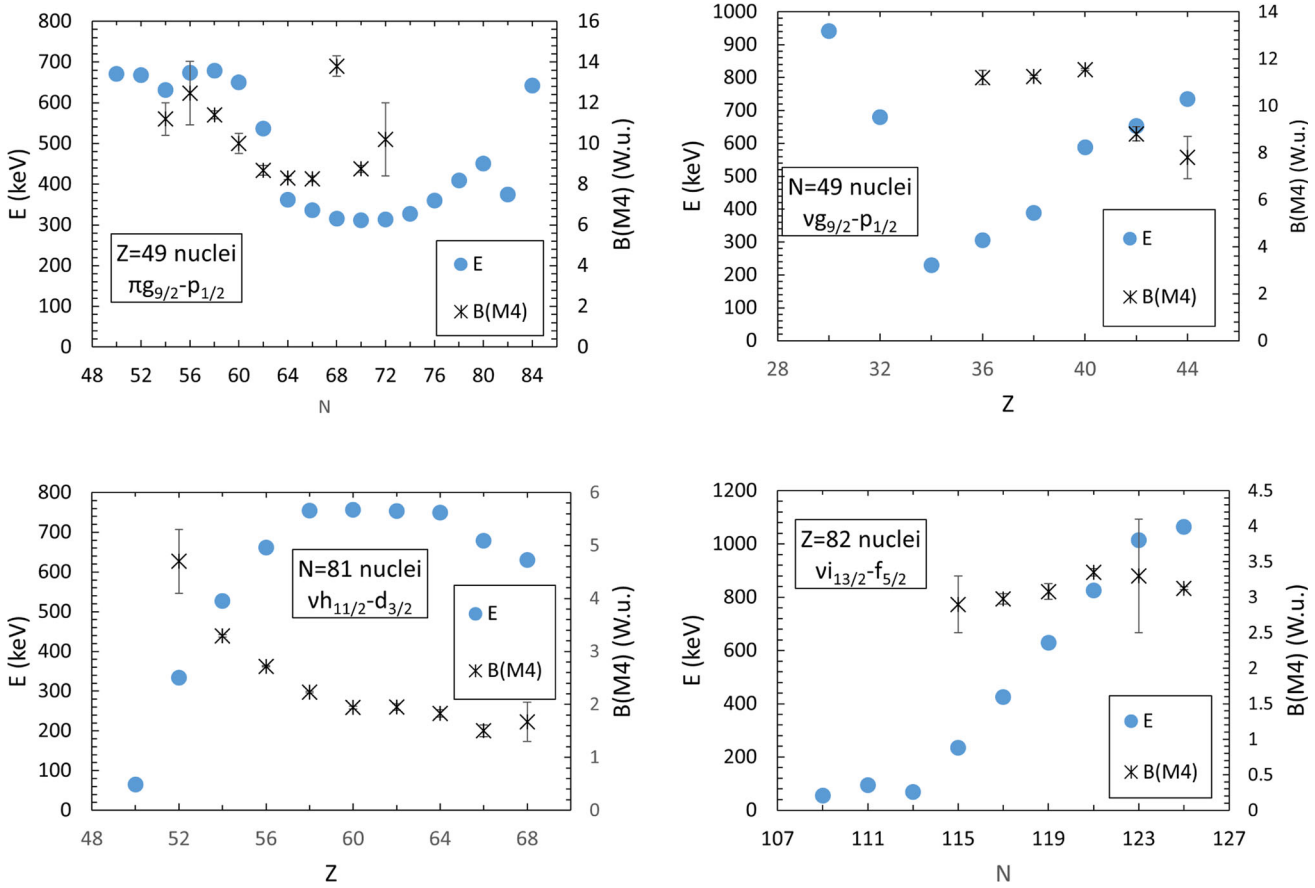

Fig. 6 Systematics of $M4$ transitions in $Z = 49$, $N = 49$, $N = 81$ and $Z = 82$ nuclei. The transition energies and transition strengths are shown. The orbital pairs mediating the $M4$ transitions are indicated

(except on the proton-rich side in ^{147}Dy, ^{149}Er where $1/2^+$ $\nu s_{1/2}$ is the ground-state). The systematics of these $\nu h_{11/2} - d_{3/2}$-mediated $M4$ transitions are shown in Fig. 6. The $B(M4)$ transition strengths decrease smoothly as proton number increases. The reduction in the $B(M4)$ strength whilst departing from $Z = 50$ is most likely due to configuration mixing. In contrast to $Z = 49$ nuclei, it seems that there is an anti-correlation between the energies and $B(M4)$ values. The change in the energy difference is shell evolution in action, and can be explained as the effect of the tensor force [27]. Above $Z = 50$, toward the heavier elements, the proton orbitals $g_{7/2}$, $d_{3/2}$, $s_{1/2}$ and $h_{11/2}$ are filled in. Filling the $j = l - 1/2$ $\pi g_{7/2}$ orbital lowers the $\nu h_{11/2}$ $j = l + 1/2$ orbital due to the attractive tensor force, and thus increasing the $h_{11/2} - d_{3/2}$ gap. Filling the $\pi h_{11/2}$ raises the $\nu h_{11/2}$ orbital due to the repulsive tensor force, thus decreasing the $h_{11/2} - d_{3/2}$ gap.

In odd-mass $Z = 82$ Pb isotopes, $13/2^+$ $\nu i_{13/2}$ isomeric states decay into the $5/2^-$ $\nu f_{5/2}$ first excited state. The systematics of these $M4$ decays are shown in Fig. 6. The $B(M4)$ values stay constant with neutron number, whilst the transition energies change significantly.

Now, we look into the wider regions, first focussing on the $\nu h_{11/2} - d_{3/2}$ transitions. In addition to $N = 81$, such transitions were observed also in the $N = 79$ and $N = 77$ isotonic chains. The systematics of the $B(M4)$ values are shown in Fig. 7. The values seem to be rather independent from the neutron number, they change in the same way with Z. There is one data point which seems to break this trend, that in $^{133}_{56}$Ba$_{77}$, where the $B(M4)$ value is lower than in the other barium isotopes. Possibly this is related to deformation and mixing in the $3/2^+$ $d_{3/2}$ dominated state (the second $3/2^+$ is only 290 keV away, much closer than in ^{135}Ba and ^{137}Ba at 588 keV and 1464 keV, respectively).

Similarly, $\nu i_{13/2} - f_{5/2}$-mediated $M4$ transitions were identified in several even Z nuclei around lead, with the systematics of the $B(M4)$ values presented in Fig. 7. The values are independent of neutron number for a given Z. In $_{84}$Po and $_{82}$Pb isotopes, the transitions seem to exhibit the same strength. In contrast, below the $Z = 82$ shell closure, the $B(M4)$ values decrease for $_{80}$Hg and even more for $_{78}$Pt. One data point seems to break the trend, at $^{201}_{84}$Po$_{117}$, with a very low $B(M4)$. There are no error bars associated to this data point in the ENSDF evaluation [28], due to the missing uncertainty on the internal decay branch. This branch should be remeasured.

A very different case is that of ^{199}Bi and ^{201}Bi. They have a $\pi h_{9/2}$ $9/2^-$ ground state and $1/2^+$ first excited state. The $1/2^+$ state has dominant intruder $\pi s_{1/2}$ configuration. The experimental $B(M4)$ values are < 0.017 W.u. (from the internal decay branch limit of 2%) in ^{199}Bi, and 0.00057(7) W.u. in ^{201}Bi. These $B(M4)$ values are much lower than any other discussed so far. This, at least partially, can be attributed to the fact that the $h_{9/2} - s_{1/2}$ $M4$ decay is l forbidden ($\Delta l = 5$). A detailed discussion can be found in [29].

$M4$ transitions were identified in deformed nuclei as well. The $T_{1/2} = 31$ y isomer in ^{178}Hf has such a decay branch. The K forbidden decay has a very low strength of $3.7 \times (5) \times 10^{-8}$ W.u., corresponding to a reduced hindrance of $f_\nu = 72(3)$ [23].

The transition strength of 95 $M4$ transitions is presented in the compilation of [30]. It was shown that all $M4$ transitions are hindered relative to the Moszkowsky estimates [31], and it advocated that for magnetic transitions, these estimates are preferable to Weisskopf units.

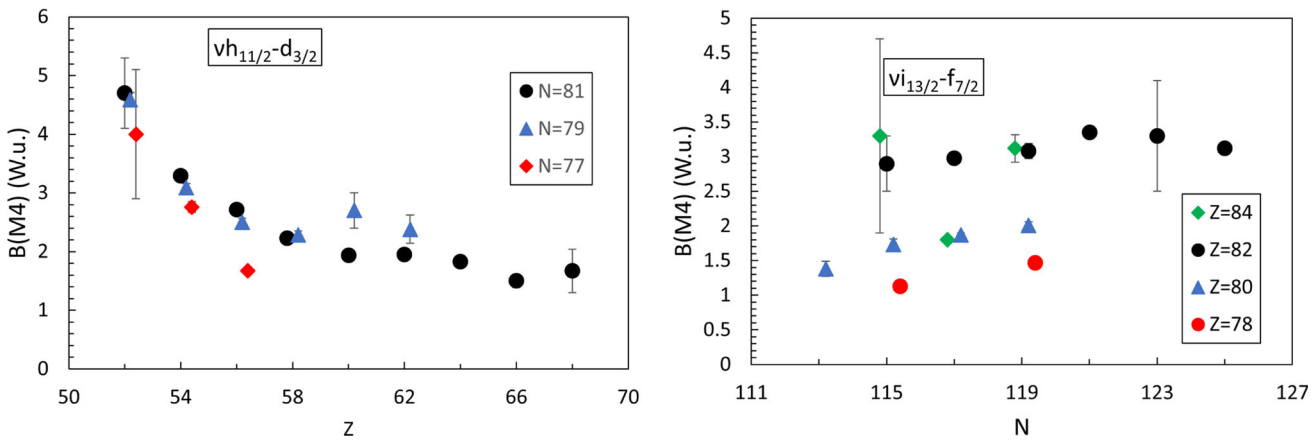

Fig. 7 Systematics of $M4$ transitions in $N = 77$, 79, 81 and $Z = 78$, 80, 82, 84 nuclei. The transition strengths are shown. The orbital pairs mediating the $M4$ transitions are indicated

5 E5 decays

In the spherical shell model, the pairs of orbitals which can give rise to $E5$ (electric triacontadipole) transitions are $h_{11/2} - s_{1/2}$ in the 50–82 shell and $i_{13/2} - p_{3/2}$ in the 82–126 one. At higher nucleon numbers, the $j_{15/2} - f_{5/2}$ pair within the N = 126–184 shell could also result in $E5$ transitions; however, no such decay has been observed so far.

$E5$ transitions mediated by the neutron $h_{11/2} - s_{1/2}$ orbital pair were observed in a number of nuclei: $^{113}Cd_{65}$, $^{117}Sn_{67}$, $^{123,125}Te_{71,73}$ and $^{137}Ba_{81}$. Here the low-energy (140–320 keV) $11/2^-$ state was observed to decay into the $1/2^+$ ground state.The $B(E5)$ transition strengths are very low, in order of 0.04-−0.05 W.u. The only exception seems to be the case of $^{133}_{56}Ba_{77}$, where a high value was reported at 10(7) W.u. [32]. This value is possibly incorrect, and it might be a consequence of the difficulty of determining the very low branching ratio at <0.1%. There are several other $11/2^-$ low-energy long-lived isomeric states in this region. However, the $3/2^+$ $\nu d_{3/2}$ state is often the ground state, consequently these isomers decay by $M4$ transitions.

Proton $h_{11/2} - s_{1/2}$-mediated $E5$ transitions were observed below $Z = 82$, in ^{207}Tl and ^{206}Tl nuclei. The transition strengths are much higher than in the case of the neutron-mediated one, at 5.0(13) W.u and 16.6(21) W.u., respectively.

Interestingly, both ^{202}Pb and ^{204}Pb have two $E5$ decays each, mediated by the $\nu i_{13/2} - p_{3/2}$ neutron-orbital pair. These are from the 9^- isomeric states with $\nu f_{5/2} i_{13/2}$ configuration. In both nuclei, the $E5$ transitions connect the isomer to the two lowest energy 4^+ levels, with transition strengths of $B(E5; 9^- \rightarrow 4_1^+)$ ∼3–4 W.u. and $B(E5; 9^- \rightarrow 4_2^+)$ ∼0.5-−0.6 W.u. This ratio as well as the $B(E4)$ from the same isomer in ^{202}Pb provides a possibility to test and refine the proton–proton residual interaction in this region.

Intriguingly, $E5$ transitions were observed in medium mass nuclei ^{90}Y and ^{90}Zr. The relatively large transition strengths of 1.66(15) W.u. and 8.74(33) W.u., respectively, are puzzling as there are no $\Delta j = 5$ orbital pairs around Z, $N = 50$. It was suggested that the 5^- isomer in ^{90}Zr as well as other 5^- states in Zr, Mo, Ru, Pd, Cd isotopes are collective states corresponding to one-phonon excitations [33]. Evidence for this comes for significant population of these states in one- and two-neutron-transfer reactions, not expected for proton-dominated states (the dominant configuration of the 5^- isomer in ^{90}Zr is $\pi g_{9/2} p_{1/2}$). Near constancy of their excitation energies and large β_5 deformation parameters are also supporting this interpretation [34].

There are $E5$ decays observed also in well-deformed nuclei. These are originating from K isomers. $E5$ decays from low-energy (< 200 keV) two-quasiparticle isomers were observed in odd-odd ^{184,186}Re and ^{192}Ir nuclei. More interestingly, there is also an $E5$ decay from the four quasiparticle high-energy 2446 keV long-lived $T_{1/2} = 31$ y metastable state in ^{178}Hf. Here the very low transition strength of $1.22(10) \times 10^{-4}$ W.u. is a consequence of K hindrance, and it corresponds to a reduced hindrance of $f_\nu = 175(11)$ [23].

6 M5, E6 and higher multipolarity decays

Only one $M5$ (magnetic triacontadipole) and one $E6$ (electric hexacontatetrapole) transition was observed to date, both in ^{53}Fe. The $19/2^-$ $T_{1/2} = 2.54(2)$ min. isomer at 3040 keV can decay by an $E6$, an $M5$ and an $E4$ transition, with energies of 3040, 1713 and 701 keV, respectively. The first direct confirmation of the $E6$ γ decay was claimed [35] very recently, in 2023. Its definitive observation needed the quantification of the sum contributions (simultaneous observation of several γ rays in the same Ge crystal adding up to the energy of 3040 keV). The relative γ-ray intensities of the $E6$, $M5$ and $E4$ transitions depopulating the isomer were determined as 0.056(17), 1.05(5) and 100, respectively. These correspond to reduced transition strengths of $B(E6) = 0.45(8)$, $B(M5) = 5.4(4)$ and $B(E4) = 0.2587(21)$ W.u. All states involved have predominantly three-valence particle character $\pi f_{7/2}^{-2} \nu f_{7/2}^{-1}$ and with the isomer at $19/2^-$, they are fully aligned. Shell-model calculations in the full fp shell were performed, and effective charges were determined. Strikingly the proton effective charges e_π for both $E4$ and $E6$ are around $0.6e$, much lower than unity. In contrast, theoretical effective charges are expected to be larger than $1e$ [36]. Note that the $E4$, $M5$ and $E6$ decays are all mediated by the $f_{7/2} \rightarrow f_{7/2}$ transition. The large $E6$ strength is the result of the large number of particles, $n = 13$, in the $f_{7/2}$ orbital. Interestingly, the corresponding $19/2^-$ state in the mirror nucleus ^{53}Co has a much shorter half-life at 247(12) ms. This is because particle decay channels are open. The first ever observation of proton radioactivity [37, 38] is from this isomeric state (the proton branch is 1.5%, with the remaining 98.5% being $\beta^+ + EC$ decay [3]).

No internal decay with multiplicity larger than six was ever observed. But they could exist. They would have enormously long partial half-lives, and they have to be in nuclei very close to stability. As indicated in Fig. 2, $M6$ transitions could be mediated by the intra-shell $i_{13/2}$-$p_{1/2}$ neutron transition. Therefore, in ^{207}Pb, the $13/2^+$ $\nu i_{13/2}$ state could decay to the $1/2^-$ $\nu p_{1/2}$ ground state by an 1633 keV $M6$ transition. This would need to compete with a 569.7 keV $M4$ to the $5/2^-$ $\nu f_{5/2}$ state. The expected branching is very small, in the order of 10^{-7}.

The most intriguing case is related to the only naturally occurring isomeric state, that is in ^{180}Ta. Whilst the 1^+ ground-state β decays with $T_{1/2} \approx 8$ h, the 77 keV 9^- isomer has an enormously long lifetime [3]. The 9^+ K isomer could decay internally by 38 keV E7 and 77 keV M8 transitions (these would be very highly electron converted), and also by both β^- and electron capture. Theoretical calculations suggest that internal $E7$ decay dominates, for which a half-life of $T_{1/2} = 8 \times 10^{18}$ years was predicted (since the decay is mainly via internal conversion electron, the partial γ-decay half-life would be much larger at 1.4×10^{31} y) [39]. The corresponding experimental limit for internal decay is $T_{1/2} > 0.63(8) \times 10^{18}$ yr (90% confidence interval) [40], still one order of magnitude shorter than the theoretically predicted value.

7 Conclusion

Isomers decaying by high multipolarity internal transitions were discussed, focussing mainly on spherical nuclei, although examples from K isomeric states were also given. The higher the multipolarity of the decay, the longer the lifetime tends to be. Therefore, $\lambda \geq 4$ decays are concentrated on and around the line of stability, as in more exotic nuclei charged particle channels would dominate. $E3$ decays in the vicinity of ^{208}Pb were discussed and they were classified depending on their single-particle origins. The chains of $M4$ and $E5$ decays next to closed shells show different behaviour in different regions. Therefore, their study within the framework of the large-scale shell model is of great interest, addressing shell evolution. In addition, comparing effective charges needed in different regions of the nuclide chart could lead to a deeper understanding of them. The highest multipolarity decays so far observed are $M5$ and $E6$, both identified from the decay of an isomeric state in ^{53}Fe. The prospect of identifying higher multipolarity decays was discussed.

Acknowledgements Fruitful discussions with Alex Brown, Magdalena Górska and Philip M. Walker are acknowledged. This work was supported by STFC (UK).

Data availability No data associated in the manuscript

References

1. S. Garg et al., At. Data Nucl. Data Tables **150**, 101546 (2023)
2. P.M. Walker, Z.S. Podolyák, Nuclear isomers, in *Handbook of nuclear physics*. ed. by I. Tanihata et al. (Springer Nature Singapore Pte Ltd., 2023)
3. ENSDF: Evaluated nuclear structure data files; www.nndc.bnl.gov/ensdf
4. P.M. Walker, Z.S. Podolyák, Phys. Scr. **95**, 044004 (2020)
5. O. Hahn, Eur. J. Inorg. Chem. **54**, 1131 (1921)
6. P. Van Isacker, M. Rejmund, Phys. Rev. Res. **4**, L022031 (2022)
7. B.A. Brown, Phys. Rev. Lett. **85**, 5300 (2000)
8. L. Morrison et al., Phys. Lett. B **838**, 137675 (2023)
9. T.A. Berry et al., Phys. Rev. C **101**, 054311 (2020)
10. E. Wilson et al., Phys. Lett. B **747**, 88 (2015)
11. O.J. Roberts et al., Phys. Rev. C **93**, 014309 (2016)
12. R. Broda et al., PRC **98**, 024324 (2018)
13. R. Broda et al., PRC **95**, 064308 (2017)
14. S.J. Steer et al., Phys. Rev. C **84**, 044313 (2011)
15. I. Bergstrom, B. Fant, Phys. Scr. **31**, 26 (1985)
16. G.D. Dracoulis, P.M. Walker, F.G. Kondev, Rep. Prog. Phys. **79**, 076301 (2016)
17. S.G. Wahid et al., Phys. Lett. B **832**, 137262 (2022)
18. I.P. Selinov, V.L. Chikhladze, D.E. Khulelidze, Izvest. Akad. Nauk SSSR, Ser. Fiz. 25, 848 (1961); Columbia Tech. Transl. 25, 857 (1962)
19. J. Blachot, Nucl. Data Sheets **11**, 1471 (2010)

20. P.M. Endt, At. Data Nucl. Data Tables **26**, 47 (1981)
21. F.G. Kondev et al., Phys. Rev. C **85**, 027304 (2012)
22. F.G. Kondev, Nucl. Data Sheets **159**, 1 (2019)
23. F.G. Kondev, G.D. Dracoulis, T. Kibédi, At. Data Nucl. Data Tables **103–104**, 50 (2015)
24. M. Mougeot et al., Nat. Phys. **17**, 1099 (2021)
25. L. Nies et al., Phys. Rev. Lett. **131**, 022502 (2023)
26. J. Park et al., Phys. Rev. C **99**, 034313 (2019)
27. T. Otsuka, Phys. Scr. **T152**, 014007 (2013)
28. F.G. Kondev, Nucl. Data Sheets **187**, 355 (2023)
29. R.A. Braga et al., Nucl. Phys. **349**, 61 (1980)
30. V.O. Sergeev, Bull. Russ. Acad. Sci. Phys. **76**, 849 (2012)
31. S.A. Moszkowski, Phys. Rev. **89**, 474 (1953)
32. Yu. Khazov, A. Rodionov, F.G. Kondev, Nucl. Data Sheets **112**, 855 (2011)
33. L.B. Horodynski-Matsushigue et al., Phys. Rev. C **60**, 047301 (1999)
34. P.E. Garrett et al., Phys. Rev. C **68**, 024312 (2013)
35. T. Palazzo et al., Phys. Rev. Lett. **130**, 122503 (2023)
36. H. Sagawa, Phys. Rev. C **19**, 506 (1979)
37. J. Cerny et al., Phys. Lett. B **33**, 284 (1970)
38. K.P. Jackson et al., Phys. Lett. B **33**, 281 (1970)
39. H. Ejiri, T. Shima, J. Phys. G **44**(6), 065101 (2017)
40. I.J. Arnquist et al., Phys. Rev. Lett. **131**, 152501 (2023)